

INTRODUCTION

It is currently not fully clear how tropical convection, cloudiness, diurnal cycle of surface temperature affect AMVs extracted from satellite imagery. Recent reports^{1,2} revealed the existence of a positive **Observation-minus-Background (O-B) speed bias** in the **tropical upper troposphere** for most satellite-channel combinations from both GEO and LEO satellites. O-B speed biases are commonly explained by erroneous altitudes assigned to AMVs. However, fast speed biases are found for AMVs that are already very high in the troposphere and it does not appear realistic to consider that they are set too low. We aim at exploring **how the dynamics and physics underlying the tropical atmosphere affect AMVs extracted from satellite imagery.**

CONCLUSIONS

- **AMV altitudes** have generally been identified as being set to **slightly too low altitudes above 400 hPa ($p < 400$ hPa; see Fig. 2 and Fig. 4).**
- **Position of tropical jet** in model and AMV appears to be in good agreement (Fig. 3).
- Better estimation of the CTH could help to improve the quality of AMVs; but an accurate **CTH estimation of thin clouds over bright desert areas remains often challenging**
- Large biases of **Metop** winds found over **boiler box** appear to be directly caused by **large & quick cloud shape changes** during the temporal gap between the two images used to track the winds (Fig. 5 and Fig. 6). The correlation methods used for wind derivation do not represent real local wind. Are winds linked to random variations of cloud shape and T_b differences?

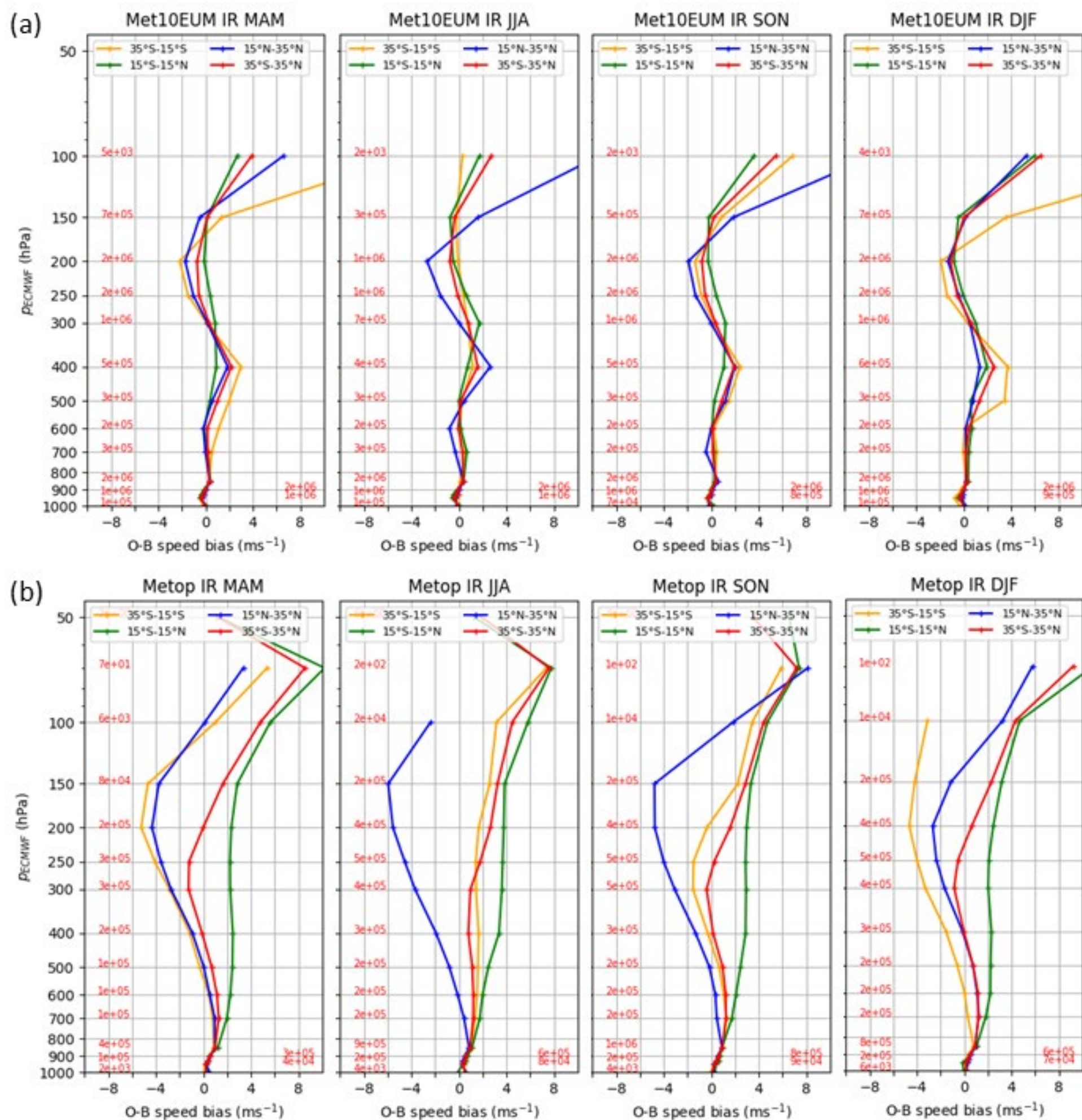


Figure 1: Profiles of seasonal O-B speed bias averaged over different latitude bands. Hourly ECMWF winds (0.5° horizontal resolution, 19 pressure levels) are compared to AMVs derived by EUMETSAT from (a) **Meteosat-10** and (b) **Metop A/B IR** imagery if $\Delta p \leq 25$ hPa.

METOP IR AMV PERFORMANCE OVER BOILER BOX

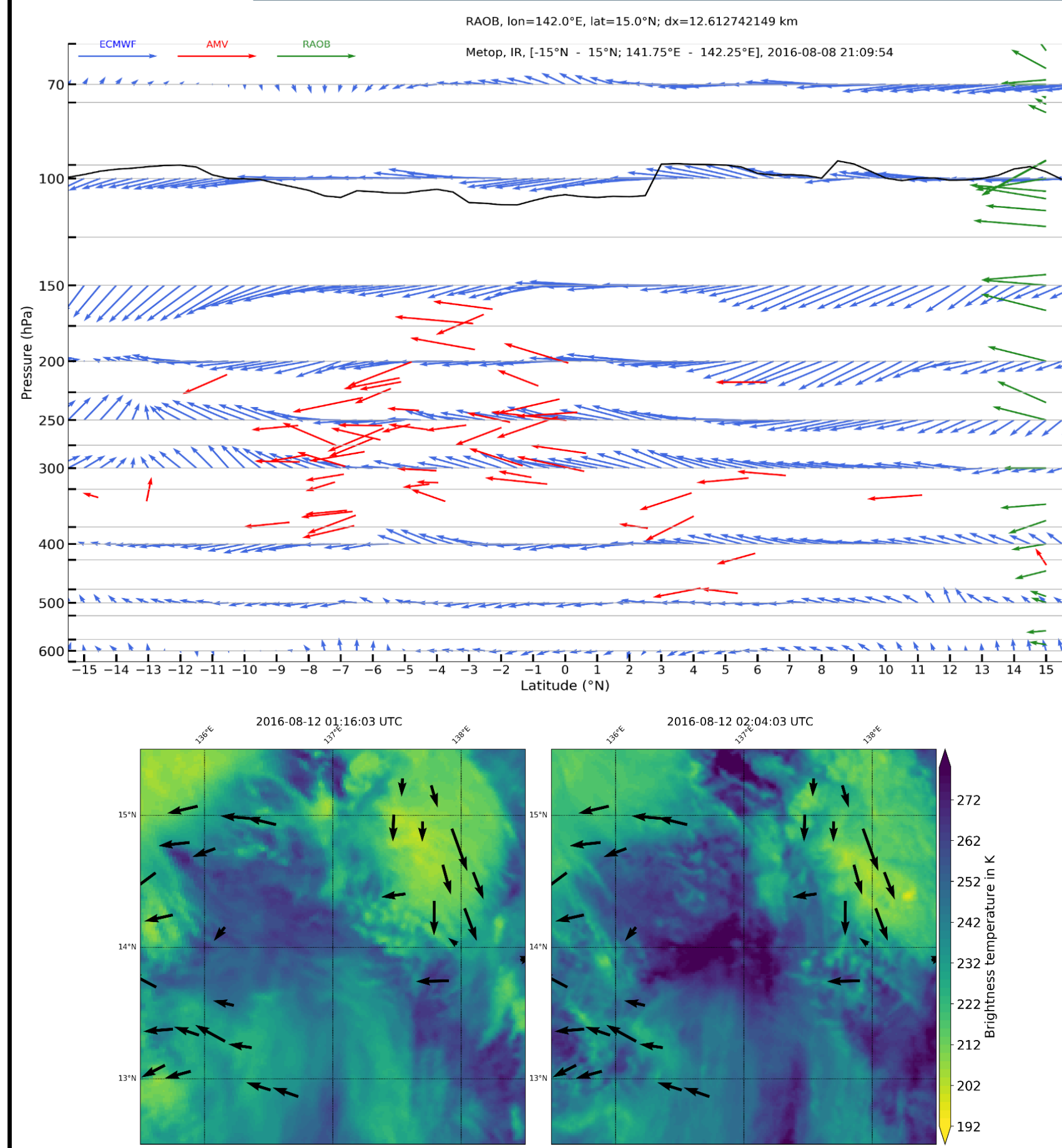


Figure 5: North-south transect of Metop AMVs (red) and ECMWF (blue) for a Metop overpass at about 142°E on 8 March, 21:09 local time. Collocated RAOB wind data at 142°E, 15°N are plotted in green.

Figure 6: Zoom on brightness temperature (T_b) field used to derive Metop winds. Dual-Metop AMVs derived from the image pair are overplotted as black arrows.

Meteosat-10 IR AMV PERFORMANCE OVER SAHARA DESERT: Position of tropical jet

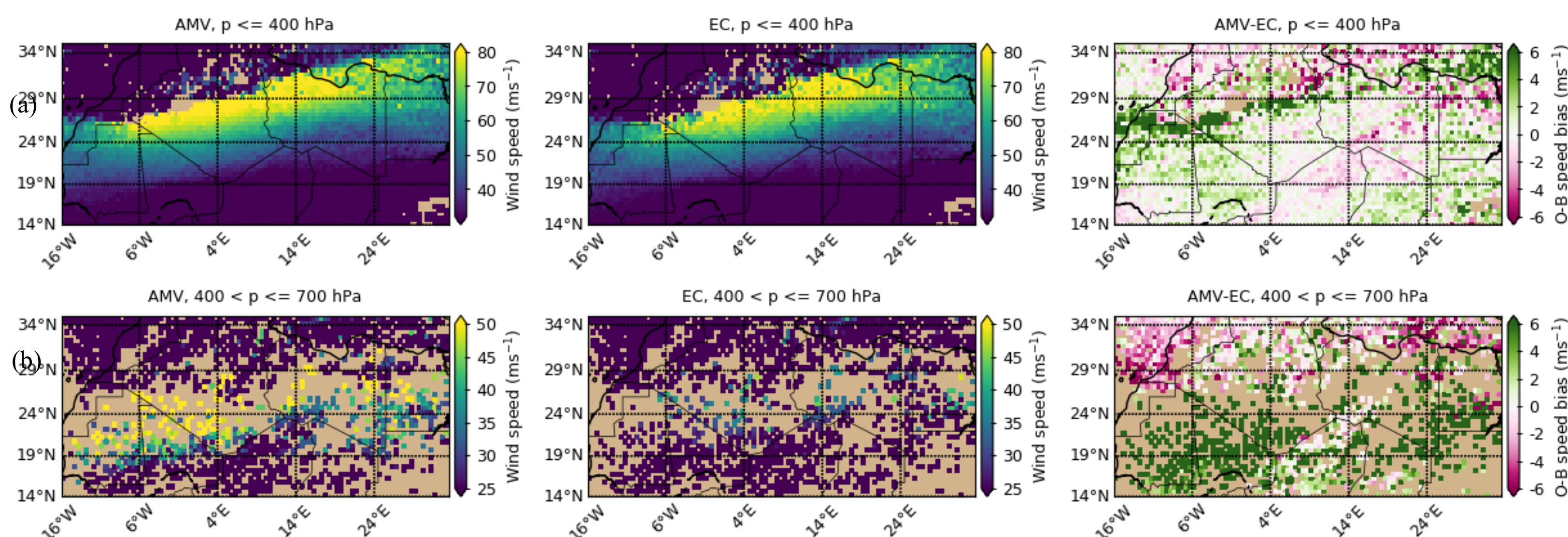


Figure 3: Wind speed averages (22.3–28.3.2016) over Northern Africa as seen by Meteosat-10 & ECMWF at (a) high- and (b) mid-level.

COMPARISON OF Met10 IR AMV TO COLLOCATED CALIPSO CTH

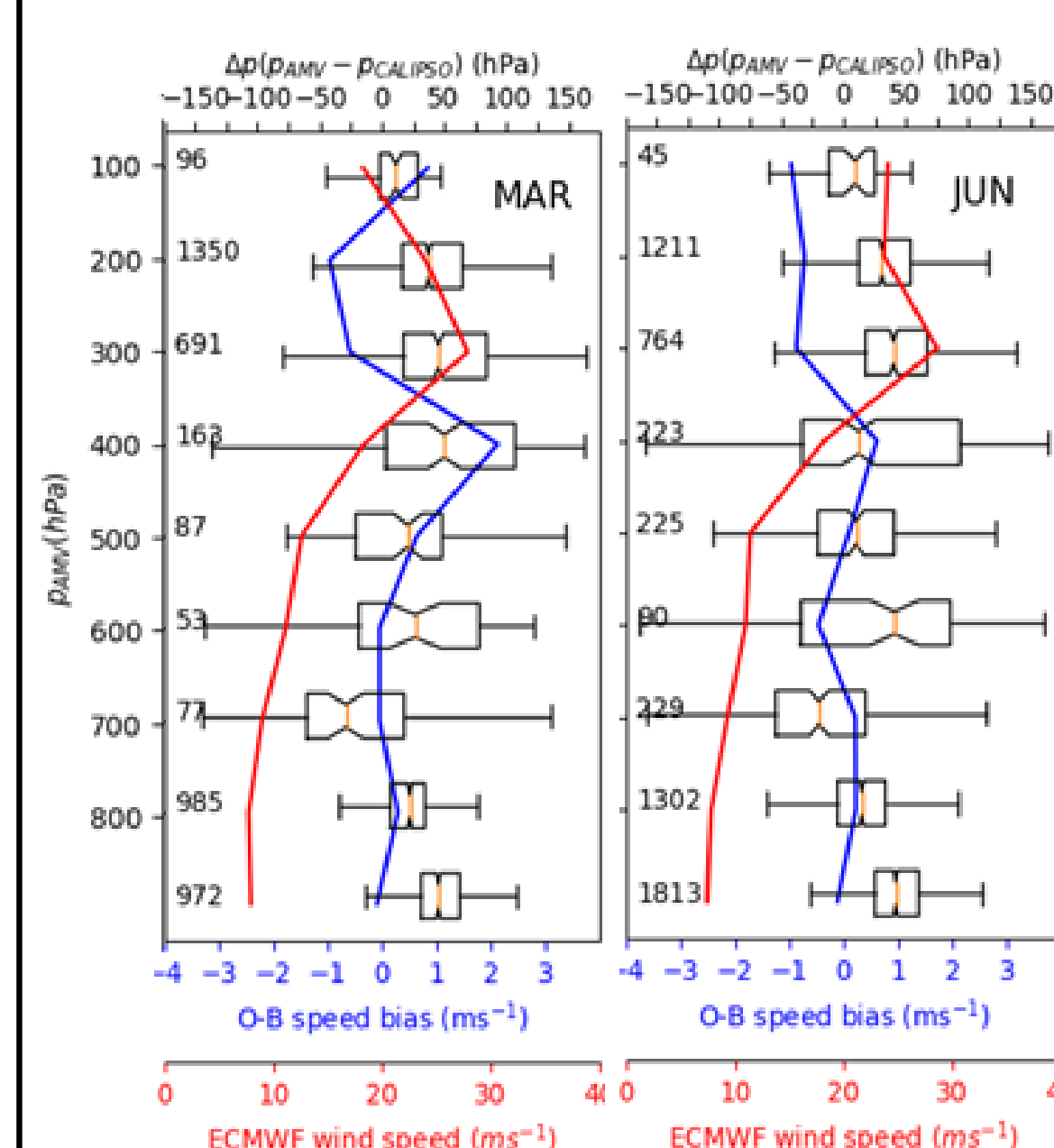


Figure 2: Box-and-whisker plots of AMV-CALIPSO pressure ($p_{AMV} - p_{CALIPSO}$) difference for different AMV pressure levels. Corresponding O-B speed bias is shown in blue, while corresponding ECMWF speeds are shown in red.

REFERENCES

- ¹Horváth, Á., O. Hautecoeur, R. Borde, H. Deneke, and S.A. Buehler, 2017: Evaluation of the EUMETSAT Global AVHRR Wind Product. *J. Appl. Meteor. Climatol.*, 56, 2353–2376. doi: <https://doi.org/10.1175/JAMC-D-17-0059>.
²Warrick, F., 2016: NWP SAF AMV monitoring: The 7th analysis report (AR7). NWP SAF Tech. Doc. NWPSAF-MO-TR-032, 35 pp.

DOWNLOAD STUDY REPORT FROM:
https://www-cdn.eumetsat.int/files/2020-11/AMV-TN-0008-TS_Final_report.pdf

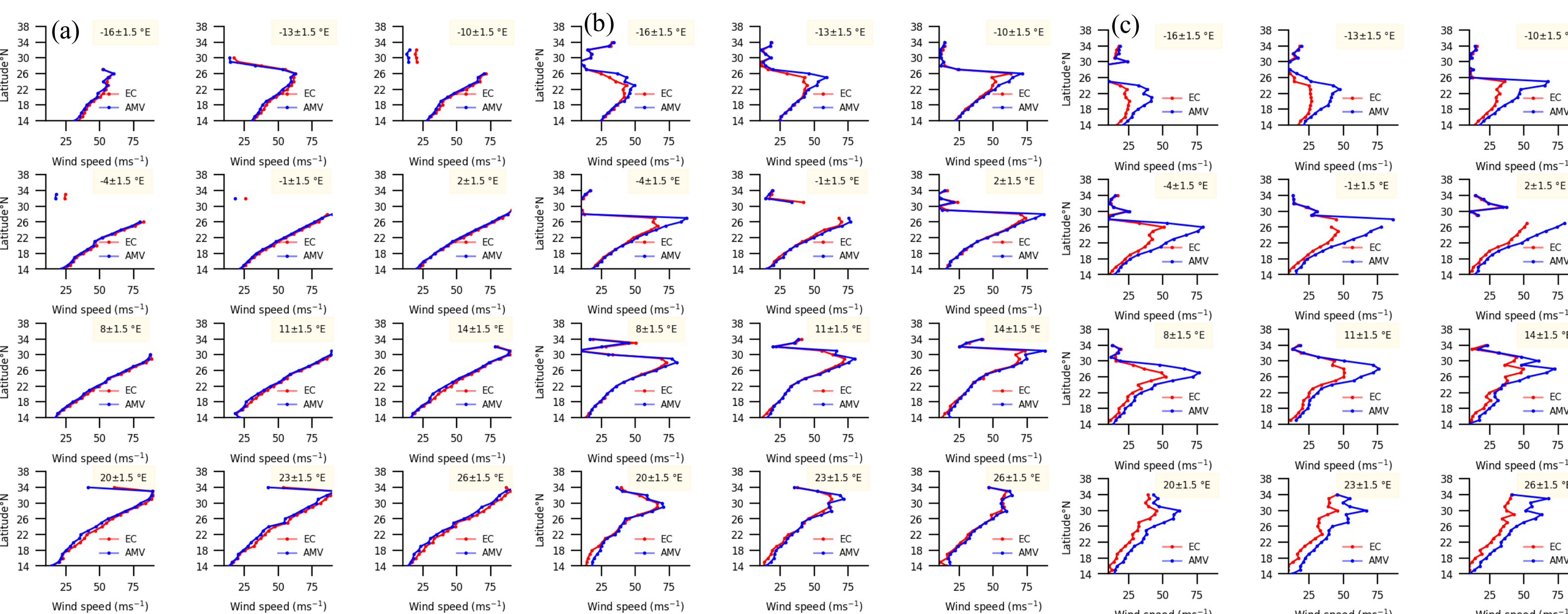


Figure 4: Observed & model winds over the Sahara desert at the (a) 200 hPa, (b) 300 hPa and (c) 400 hPa level. Wind speeds are averaged from 22.3 - 28.3.2016 and over $\pm 1.5^\circ$ longitude bands. ECMWF winds are depicted in red, Meteosat-10 IR AMV in blue.